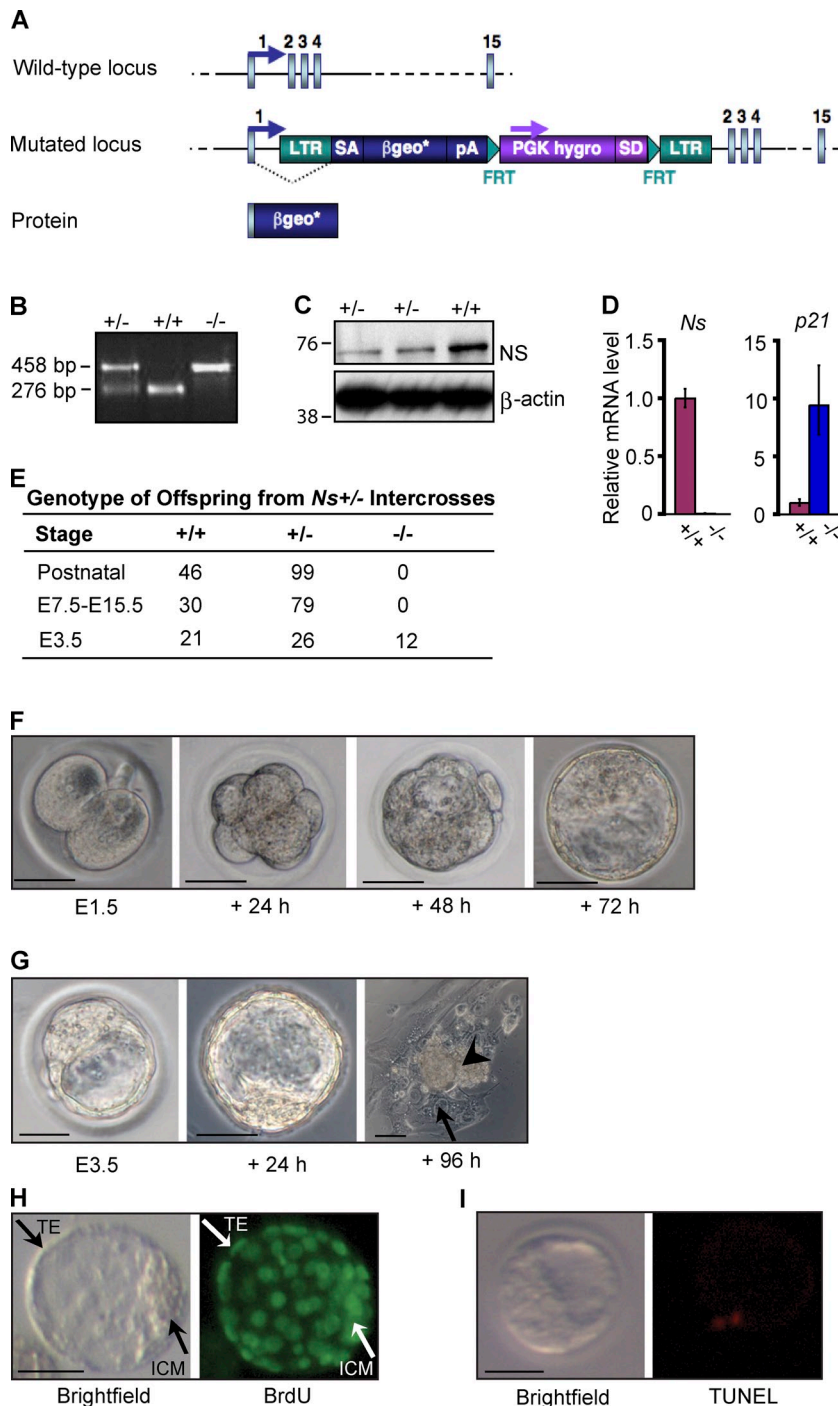


Qu and Bishop, <http://www.jcb.org/cgi/content/full/jcb.201103071/DC1>Figure S1. **Disruption of the nucleostemin gene by means of gene trap mutation.**

(A) Schematic of wild-type *Ns* locus, the mutated locus carrying the gene trap insertion in ESC line S4-4B1 (see Materials and methods), and the predicted fusion protein. The *Ns* genomic locus contains 15 exons (boxed). Arrows indicate the transcription start and direction. The gene trap insertion was further mapped in the present study as 860 bp downstream of exon 1 in the intron 1 region of the *Ns* locus. The insertion creates a null allele of *Ns*, producing a fusion transcript encoding the first four amino acids of the NS protein and the reporter protein β -galactosidase-neomycin phosphotransferase (β geo*) under the control of the endogenous *Ns* gene regulatory elements. (B) Genotype analysis of preimplantation embryos by PCR and gel electrophoresis. To genotype embryos derived from *Ns*^{+/−} intercrosses, two rounds of PCR amplification using nested primers were performed on genomic DNA extracted from individual embryos as described in Materials and methods. The bands at 276 bp and 458 bp represent the wild-type allele and the gene trap allele of *Ns*, respectively. The sizes of the bands conform to predictions based on the PCR primers. (C) Western analysis of *Ns*^{+/−} MEFs derived from E13.5 embryos demonstrating the decreased levels of NS protein expression compared with littermate wild-type controls (top), which is consistent with the disruption of the *Ns* locus by the gene trap mutation. β -Actin expression was analyzed as a loading control (bottom). The positions of molecular mass standards (in kilodaltons) are shown. (D) QPCR analysis of *Ns* and *p21* expression in E2.5 preimplantation embryos, using primers corresponding to regions in exons 13–14 of the *Ns* allele. Total RNA from three litters of single embryos derived from *Ns*^{+/−} intercrosses was isolated and analyzed as described in Materials and methods. Each litter contained embryos that exhibited nondetectable *Ns* expression and were thus considered presumptive *Ns*-null embryos (*Ns*^{−/−}). Shown are representative data comparing the presumptive littermate *Ns*^{+/+} and *Ns*^{−/−} embryos. The data were normalized to the expression of *Gapdh* and were the average of experimental triplicates, represented as mean \pm SEM. The data are displayed relative to results with the presumptive wild-type control. (E) NS deficiency results in embryonic lethality. Genotypes were determined for postnatal or embryonic mice derived from *Ns*^{+/−} intercrosses. *+/+*, wild-type mice; *+/−* (*+/βgeo*), heterozygous mice; *−/−* (*βgeo/βgeo*), homozygous knockout mice. (F–I) Embryos were isolated from *Ns*^{+/−} intercrosses and analyzed. *Ns* heterozygotes do not exhibit any overt phenotype distinguishable from wild-type controls in the analyses of morulation and blastulation during in vitro culture of E1.5 embryos (F), outgrowth culture of E3.5 embryos (G), BrdU incorporation by E3.5 embryos (H), and TUNEL staining of E3.5 embryos (I). The panels are related to C, D, E, and F in Fig. 1, respectively. A littermate *Ns*^{+/−} embryo is illustrated for each assay. The arrow and arrowhead in G indicate trophoblast giant cells and ICM-derived cells, respectively. Bars, 40 μ m.



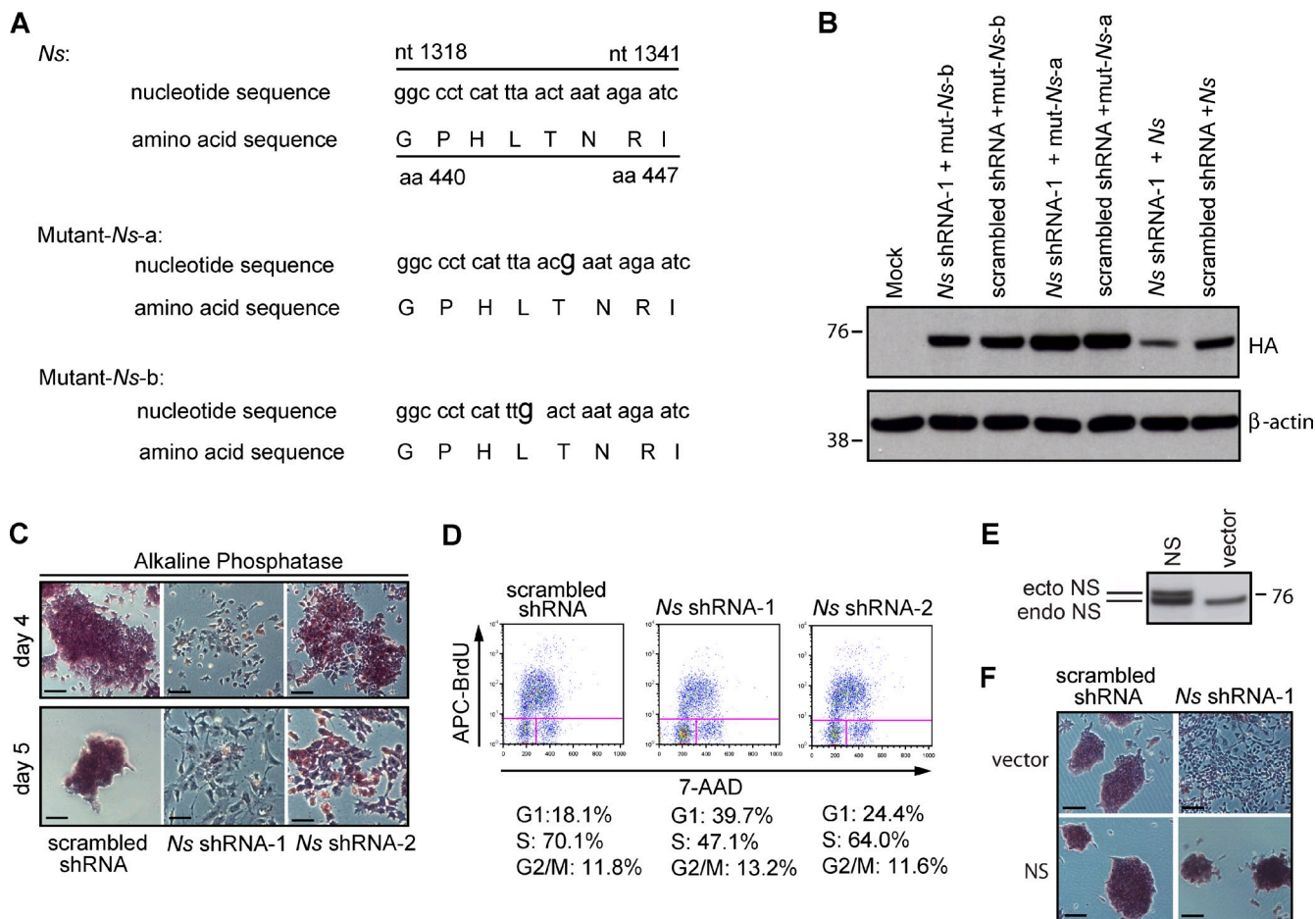


Figure S2. Evaluation of the specificity of *Ns* shRNA. (A and B) Two *Ns* constructs with different point mutations prevent knockdown of NS by an shRNA (*Ns* shRNA-1 as below) directed against the wild-type allele of *Ns*. (C and D) The effects on ESC cell cycle and differentiation correlate with the degree of NS knockdown using two shRNA constructs targeting different regions of the *Ns* transcript. (E and F) Ectopic expression of human NS impeded the differentiation normally imposed by KD of the intrinsic mouse NS. (A) Two mutant versions (mut) of mouse *Ns* cDNAs that could not be targeted by the *Ns* shRNA-1. Two nucleotides (nt) were mutated as shown in mutants *Ns*-a and b, but the amino acid (aa) sequences remained unchanged. Both the wild-type and mutant *Ns* were tagged with an HA epitope and cloned in the pCMV-HA vector. (B) Western analysis of 293T cells 3 d after transfection with the indicated expression vectors. The two different point mutations in the target sequence for *Ns* shRNA-1 prevented KD of NS. The HA tags for mutant and wild-type NS proteins could be detected when cells were cotransfected with scrambled shRNA. *Ns* shRNA-1 could not suppress the overexpression of mutant *Ns*, but was able to diminish wild-type HA-tagged NS protein. β -Actin expression was analyzed as a loading control. The positions of molecular mass standards in B and E (in kilodaltons) are shown. (C) Representative morphology and AP staining of ESCs 4 and 5 d after transfection with either *Ns* shRNA-1 or shRNA-2, which have different target sequences in *Ns* RNA. The two *Ns* shRNAs induced differentiation of ESCs, and there was a direct correlation between the level of NS KD and the extent of the phenotypic response. By d 4 after transfection, cells that had received *Ns* shRNA-1 exhibited morphological differentiation and the majority had lost staining for AP. Cells that had received *Ns* shRNA-2 also became flattened and lost the stereotypical colony morphology, but exhibited residual AP staining, indicative of a less differentiated phenotype compared with cells with shRNA-1. By d 5, the cells with *Ns* shRNA-2 had become more dispersed, but remained positive for AP activity. See Fig. 2 C for quantifications and illustrations of undifferentiated, partially differentiated, and fully differentiated colonies of ESCs 5 d after the respective transfections. The KD of NS by shRNA-2 was less efficient than that by shRNA-1. See Fig. 2 A for details. (D) Cell cycle profiles of asynchronously growing ESCs 4 d after transfection with either *Ns* shRNA-1 or shRNA-2. The percentages of cells in particular phases of cell cycle are shown. The effect on cell cycle induced by the two *Ns* shRNAs also correlates with the level of NS KD. Both shRNAs reduced the fraction of cells in the S phase and increased the fraction in G1, but the effect of *Ns* shRNA-1 was more robust than that of shRNA-2. Depletion of NS reconfigures the ESC cell cycle, as illustrated here. See Results and Fig. 2, H–J, for details. (E) Western analysis of endogenous mouse NS (endo NS) and ectopic human NS (ecto NS) in ESCs. The ectopic human NS did not contain a matched target sequence for the *Ns* shRNA (shRNA-1) used in the experiment. Stable ESC lines ectopically expressing human NS in the pCAG vector were generated as described in Materials and methods and were used for the analysis. The mouse and human NS were detected by the same antiserum, but the human form can be distinguished from the mouse because of its larger size. (F) Representative morphology and AP staining of stable ESC lines 4 d after transfection of the indicated shRNAs. Ectopic expression of human NS, which could not be recognized by *Ns* shRNA-1, prevented the differentiation of ESCs in response to the shRNA. Bars, 100 μ m.

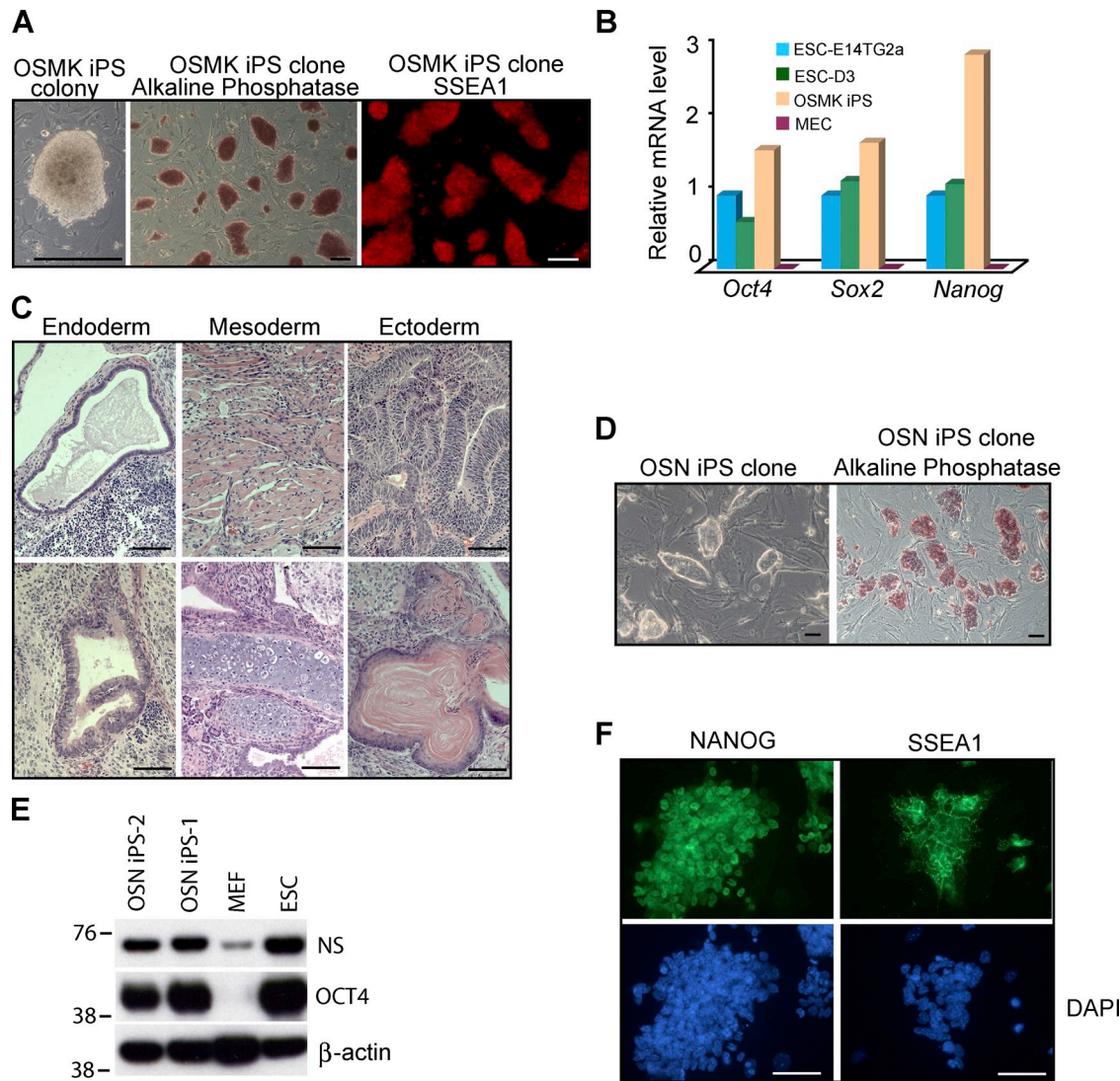


Figure S3. Reprogramming of mouse mammary epithelial cells and embryonic fibroblasts. (A–C) Reprogramming of MECs with a combination of *OCT4*, *SOX2*, *MYC*, and *KLF4*. MECs were transduced with retroviruses encoding the combination of OSMK, cultured in standard ESC media for 4 d, and then maintained in knockout serum replacement-based ESC media. Small colonies resembling those of ESCs appeared as early as 7 d after transduction and increased 10–20-fold by 3–4 wk after transduction (not depicted). Colonies identified by morphological criteria as resembling ESCs were isolated and expanded in standard ESC media as clones after 3 wk. The MEC reprogramming efficiency (see Table S3) and kinetics appeared comparable to those reported previously for other somatic cell types. (A) Morphology of primary OSMK iPS colony (colony) 7 d after transduction and the established OSMK iPS cells (clone). The latter stained positive for AP activity and with antibody against SSEA1. (B) QPCR analysis demonstrating reactivation of endogenous pluripotency markers *Oct4*, *Sox2*, and *Nanog* in OSMK iPS cells when compared with normal ESCs (E14TG2a and D3), using primers detecting the mRNA for the endogenous mouse genes but not that for the transduced human cDNAs. The MECs that were used to generate the iPS cells were analyzed as a control. Results were normalized to the expression of *Gapdh*. The data are displayed relative to results with E14TG2a and represent the average of triplicate QPCR analyses. One of three independent experiments with comparable results is shown. (C) Hematoxylin and eosin staining of teratomas generated from OSMK iPS cells. Shown is a teratoma containing endoderm (respiratory epithelium and gut-like epithelium, top and bottom of left panel, respectively), mesoderm (muscle and cartilage, top and bottom of middle panel, respectively), and ectoderm (neural tissue and epidermis, top and bottom of right panel, respectively), providing evidence of ESC-like properties. (D–F) Reprogramming of MEFs with a combination of *OCT4*, *SOX2*, and *NS*. MEFs were transduced with retroviruses encoding the combination of OSMK, cultured in standard ESC media for 4 d, and then maintained in knockout serum replacement-based ESC media. ESC-like colonies were picked at 6–8 wk post-transduction and expanded in standard ESC media. (D) Morphology and AP staining of established OSN iPS cells. (E) Western analysis of NS and OCT4 proteins in OSN iPS cells, normal ESCs (E14TG2a), and the MEFs that were used to generate the iPS cells. β -Actin was used as a loading control. The antibodies used could recognize both human and mouse homologues, but the data likely represent only endogenous proteins due to silencing of the retroviral vectors. The positions of molecular mass standards (in kilodaltons) are shown. (F) Expression of pluripotency markers (NANOG and SSEA1) in OSN iPS cells, as assessed by immunofluorescence microscopy. Nuclei were counterstained with DAPI. Bars, 100 μ m.

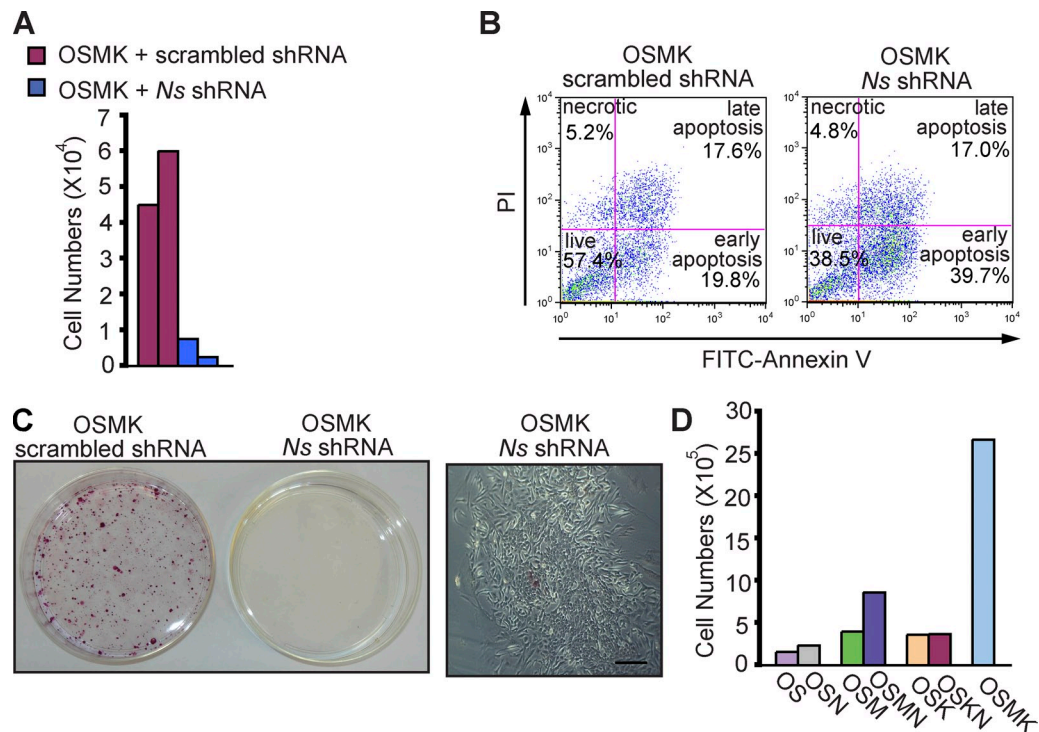


Figure S4. Intrinsic *Ns* is required for the reprogramming of somatic cells to pluripotency by ectopic factors. (A) Cell proliferation. Approximately $3 \times 10,000$ MECs were transduced with retroviruses expressing reprogramming factors OSMK and lentiviruses expressing the indicated shRNAs. The number of cells in duplicate samples was counted 5 d later. For A–C, *Ns* shRNA-1 was used for depletion of *NS*. (B) Apoptosis assay. 5 d after the indicated transductions, MECs were stained with Annexin V and propidium iodide (PI) and then quantified by FACS analysis. Cells that are in early apoptosis are Annexin V positive and PI negative. Cells that are in late apoptosis or already dead are both Annexin V and PI positive. (C) Formation of AP-positive colonies by MECs after the indicated transductions. Approximately 100,000 cells from each sample were replated into iPS cell medium in 10-cm plates 4 d after transduction and analyzed 21 d after the transduction. Phase image of a cluster of flattened cells in samples with OSMK and *Ns* shRNA-1 is shown on the right. Bar, 100 μ m. (D) The effect of ectopic expression of *NS* on proliferation of MECs transduced with reprogramming factors. Approximately 100,000 MECs were subjected to the indicated transductions and subsequently plated in media suitable for iPS cell induction. Shown are the averages of cell numbers of duplicate samples counted 12 d after transduction.

Table S1 is provided as an Excel file and contains the complete expression array dataset for the *NS* knockdown cells vs. controls with scrambled shRNA (Ctl) comparison. Shown are the identifying information and statistics including gene name, description, average log intensities (Mean), log2-fold changes (log2FC), adjusted P-value (AdjP), false discovery rate (FDR), Bayes factor (B), and Gene Ontology (GO).

Table S2 is provided as an Excel file and includes all genes found to be significantly up-regulated or down-regulated by expression array analysis in *NS* knockdown cells (adjusted P-value < 0.05). Annotations are as in Table S1.

Table S3. **Reprogramming of mammary epithelial cells to induced pluripotent stem cells**

Combinations					Timing of ESC-like colonies	Establishment of iPS cell lines (estimated frequency)
4 factors	OCT4	SOX2	MYC	KLF4	1–2 wk	Yes (~0.05%)
	OCT4	SOX2	MYC	NS	2–3 wk	Yes (~0.05%)
	OCT4	SOX2		KLF4	NS	Yes (~0.04%)
	OCT4		MYC	KLF4	NS	No
		SOX2	MYC	KLF4	NS	No
3 factors	OCT4	SOX2			NS	Yes (~0.01%)
	OCT4	SOX2		KLF4		Yes (~0.02%)
	OCT4	SOX2	MYC			Yes (not determined)
	OCT4		MYC	KLF4		No
	OCT4		MYC		NS	No
	OCT4			KLF4	NS	No
		SOX2	MYC	KLF4		No
		SOX2	MYC		NS	No
		SOX2		KLF4	NS	No
2 factors	OCT4	SOX2				No
	OCT4		MYC			No
	OCT4			KLF4		No
	OCT4				NS	No
		SOX2	MYC			No
		SOX2		KLF4		No
		SOX2			NS	No

Summary of factor combinations used for reprogramming of MECs, timing of emergence of ESC-like colonies, establishment of iPS cell lines, and estimated reprogramming efficiency. MECs were transduced with various combinations of reprogramming factors. Colonies identified as resembling ESCs by morphological criteria were isolated and expanded after either 3 wk (OSMK) or 6 wk (all other combinations). The reprogramming efficiency was calculated as the number of established iPS cell lines divided by number of cells infected with desired combinations of factors as described in Materials and methods.